Different Types of Nanosized Carbon Materials Produced by a Metal Dusting Process

ARTICLE *in* THE JOURNAL OF PHYSICAL CHEMISTRY C · DECEMBER 2008

Impact Factor: 4.77 · DOI: 10.1021/jp803202m

3 AUTHORS, INCLUDING:

Jeng-Kuei Chang
National Central University
131 PUBLICATIONS **2,147** CITATIONS

SEE PROFILE

Article

Different Types of Nanosized Carbon Materials Produced by a Metal Dusting Process

Jeng-Kuei Chang, Heng-Yi Tsai, and Wen-Ta Tsai

J. Phys. Chem. C, **2008**, 112 (51), 20143-20148 • Publication Date (Web): 02 December 2008

ARTICLES

Different Types of Nanosized Carbon Materials Produced by a Metal Dusting Process

Jeng-Kuei Chang,* Heng-Yi Tsai, and Wen-Ta Tsai

Department of Materials Science and Engineering, National Cheng Kung University, 1 University Road, Tainan City 701, Taiwan

Received: April 14, 2008; Revised Manuscript Received: October 30, 2008

Preparation of carbon nanorods, multiwall nanotubes, single-wall nanotubes, and nanoballs, depending on reaction conditions, is demonstrated by a metal dusting process, in which a blasted 304 L stainless steel coupon and $CO-CO_2$ mixed gas are reacted in the 500−800 °C temperature range. During the process, fresh Fe−Ni nanoparticles, which catalyze formation of the nanosized carbon materials, are produced spontaneously. This process is simple and easily scaled up; therefore, mass production of the nanosized carbon materials is realizable. The formation mechanism for each nanostructure is also proposed in this paper.

1. Introduction

Nanosized carbon materials, especially carbon nanotubes (CNTs) that were discovered by Iijima in 1991,[1] have attracted a lot of attention because of their unique physical and mechanical properties.[2,3] The potential applications of nanosized carbon materials are widespread in many fields, such as field emission sources,[4] electric nanoconductors,[5] Li ion secondary batteries,[6] electric double-layer capacitors,[7] fuel cells,[8] hydrogen storage systems,[9] and molecular sieves.[10] Various synthetic methods have been developed to produce CNTs, including arc discharge,[11] laser ablation,[12] and chemical vapor deposition (CVD).[13] Finding a better preparation process with a potential for mass production of various nanosized carbon materials is of great importance and interest.

Metal dusting is a catastrophic form of corrosion, which leads to disintegration of Fe-, Co-, and Ni-based alloys into a powdery mixture of graphite and metal dusts. These nanosized metal dusts can catalyze the deposition of carbon from a strongly carburizing atmosphere with high carbon activity (a_C).[14−16] However, neither the feasibility of preparing different structures of nanosized carbon materials from metal dusting nor their detailed formation mechanism has been explored in the literature. Initial investigations by Hochman[17] and studies by Grabke et al.[18−20] and by Chun et al.[21−23] have unraveled the metal dusting mechanisms of pure metals and alloys in the 400−800 °C temperature range. Briefly, the reaction mechanism of metal dusting for stainless steels, proposed by Grabke,[20] proceeds in the following sequence of steps: (i) Carbon is transferred from the carbon-supersaturated environment to the steel surface through local defects in the oxide film and dissolves in the steel. (ii) The dissolved carbon diffuses inward and causes internal precipitation of stable carbide, $M_{23}C_6$ and/or M_7C_3, consisting mainly of Cr. (iii) Upon further carbon transfer, metastable carbide, M_3C (Fe is a major species in M), forms on the internal carbide. (iv) Due to the low carbon diffusivity in M_3C, graphite nucleates and grows on the sample surface upon carbon deposition. (v) The decomposition of M_3C is triggered by graphite deposition, which decreases the a_C at the M_3C/graphite interface to unity. The carbon atoms attach to the basal planes of the deposited graphite, which grows into the sample surface; the metal atoms diffuse outward through the graphite layers and agglomerate to nanosized particles. (vi) These metallic nanoparticles act as catalysts for formation and growth of nanosized carbon materials. Further carbon deposition from the atmosphere makes the above steps repeat indefinitely. It should be emphasized that although the corrosion reaction beneath the metal surface has been extensively studied, little information about the characteristics of the deposited nanosized carbon materials is known.

The metal dusting process is expected to be an efficient route to prepare nanosized carbon materials since it is quite simple; besides the reaction gas, a bulk of steel is the only substance needed. Large-scale production should be achievable. Most importantly, fresh catalyst nanoparticles are constantly provided during the process; therefore, a high yield of deposited carbon is anticipated. Grabke[20] has indicated that the metal wastage rate (weight loss per unit area and time period) and carbon deposition rate for several selected systems are approximately 1 mg/cm^2·h and 10 mg/cm^2·h, respectively, at 600 °C. In this study, we demonstrate that different types of nanosized carbon materials, including nanorods, multiwall nanotubes, single-wall nanotubes, and metal encapsulated nanoballs, can be prepared by exploiting the metal dusting process of a 304 L stainless steel under proper reaction conditions. The formation mechanism for each nanostructure is also proposed.

2. Experimental Methods

304 L austenitic stainless steel coupons with dimensions of 10 mm × 10 mm × 1 mm were obtained from Gloria Material Technology Corp. The chemical composition of the steel was analyzed with a glow discharge spectrometer [GDS, with a parts per billion (ppb) level of accuracy]; the analytical data are shown in Table 1. The coupons were first blasted for 30 s by Al_2O_3 powders, which had a particle size in the range of 200−250 μm. The surface oxide on the steel coupons was physically removed. After an ultrasonic cleaning, no Al_2O_3 remained on the coupons. GDS analyses confirmed that the surface chemical

* Corresponding author: telephone +886-6-2757575, ext 62942; fax +886-6-2754395; e-mail catalyst@mail.mse.ncku.edu.tw.

10.1021/jp803202m CCC: $40.75
Published on Web 12/02/2008

TABLE 1: Chemical Composition of the 304 L Stainless Steel Used in This Study

element	C	Cr	Ni	Si	Mn	Cu	S	P	Fe
wt %	0.026	17.92	8.12	0.46	1.19	0.12	0.002	0.04	72.12

composition (except oxygen) of the steel did not change after the blasting; no elemental enrichment was found. The blasted samples were placed into a tube furnace, which was flushed with inert argon gas before $CO-CO_2$ mixed reaction gas (the volume ratio was 35:1) was introduced. The temperature was then ramped to 500, 600, 700, and 800 °C, respectively, and held for 30 h. The gas flow rate was 60 sccm, and the pressure in the reaction chamber was 1 atm. The carbon activity (a_C) of the atmosphere can be calculated according to the following reaction:

$$2CO_{(g)} = C + CO_{2(g)} \quad (1)$$

with $a_C = (P_{CO})^2 K/P_{CO_2}$, where P_{CO} and P_{CO_2} are the partial pressures of carbon monoxide and carbon dioxide, respectively, and K is the equilibrium constant. The a_C of the $CO-CO_2$ mixed gas at 500, 600, 700, and 800 °C was 9250, 440, 39, and 5, respectively. Afterward the samples were cooled down to room temperature in argon gas to avoid further carbon deposition. The typical weight gain of the steel coupon, which was attributed to carbon deposition and also to substrate oxidation, exposed at 500 °C was 2 mg/cm^2, but it increased to approximately 4 mg/cm^2 at 800 °C.

Surface morphologies of the specimens were examined with a scanning electron microscope (SEM, Philip XL-40). The nanosized carbon materials deposited on the steel coupons were then detached from the substrates with a knife and dispersed in ethyl alcohol (99.5%) with ultrasonic sonication (for 5 min) before they could be collected on a Cu grid, which was covered with a lacy carbon film. The microstructures of the deposited carbon were then further analyzed with a high-resolution transmission electron microscope (HRTEM, FEI Tecnai F20) operated at 200 kV.

3. Results and Discussion

Figure 1 panels a−d show the surface morphologies of the 304 L stainless steels after being exposed in $CO-CO_2$ mixed gas for 30 h at 500, 600, 700, and 800 °C, respectively. These SEM micrographs reveal that the sample surfaces are covered with nanosized carbon materials, but their characteristics clearly depend on the reaction temperatures. At 500 °C, lots of short and twisted carbon filaments can be observed; their average diameter is approximately 80 nm and the length is typically less than 500 nm. Metal particles, which were produced from the metal dusting process, can be clearly observed as bright spots on the top of the filaments. Accordingly, the tip-catalyzed growth model of the carbon filament is suggested in this case.[24] At 600 °C, the produced carbon filaments are straighter and much longer (they are a few micrometers in length) than those formed at 500 °C. The average diameter of the filaments is about 60 nm. At 700 °C, there is a cobweblike structure on the sample surface. As can be seen, the carbon network is composed of numerous extremely fine filaments (diameter of around 10 nm). At 800 °C, many thick carbon sticks with rough surfaces can be found; each has a diameter of up to 200 nm and a length of several micrometers. As shown in Figure 1, the high uniformity and large amount of deposited carbon obtained at various reaction temperatures indicate a possibility of preparing various types of nanosized carbon materials via the metal dusting process.

The microstructure of the nanosized carbon materials produced at various temperatures can be further characterized by HRTEM. Figure 2a shows the micrograph of the carbon filament formed at 500 °C; a solid and curved carbon nanorod can be clearly observed. As revealed in the high-magnification image (Figure 2b), the short-range ordered carbon layers randomly grew in the rod; they are even perpendicular to one another. In addition, some amorphous regions were also present inside. Figure 2c shows a tip region of a carbon rod where a catalyst particle with a diameter of 70 nm has fallen away. Baker et al.[25,26] have indicated that the exothermic decomposition reaction of carbon feedstock gas on the front surface of a catalyst caused a temperature gradient across the particle; this driving force made the deposited carbon atoms dissolve and diffuse through the particle and is precipitated on the rear side of the catalyst to form the carbon filament. Nielsen and Trimm[27] further proposed that a concentration gradient of carbon also occurred across the catalyst since oversaturation of carbon existed on the front surface of the particle where the feedstock gas was decomposed and carbon was absorbed. At 500 °C, with such a high a_C (i.e., 9250) of reaction atmosphere, the carbon deposition tendency (and thus the deposition rate[28]) from the atmosphere is huge. Thereby, both gradients of temperature and carbon concentration across the catalyst particle are large, and so is the carbon precipitation rate behind the catalyst. Accompanied with the relatively low reaction temperature, when carbon atoms do not have sufficient energy and mobility to arrange themselves, a solid nanorod with poor crystallinity is thus formed. In addition, due to the large diffusion gradient, the deposited carbon on the front surface of the catalyst was quickly and completely transferred to the rear side; therefore, as revealed in Figure 2c, the metal particle was not fully surrounded by carbon layers. As a result, the catalyst particle was separated from the nanorod during ultrasonic sonication (for the TEM sample preparation).

Figure 3a shows the HRTEM photo of the nanosized carbon material prepared at 600 °C. A multiwall CNT with outer and inner diameters of 60 and 20 nm, respectively, can be observed. The chemical composition of the catalyst particle on the tip of the multiwall CNT was analyzed with an auxiliary X-ray energy-dispersive spectroscope (EDS), equipped on the HRTEM. The analytical result showed that the metallic particle had 89 wt % Fe and 11 wt % Ni. However, no Cr was detected within the particle (it should be 18 wt % in the 304 L substrate, as shown in Table 1), since it could be fixed by the formation of spinel oxide and/or stable carbide near the sample surface.[23] The enlarged micrograph of the wall of the CNT (Figure 3b) shows that the long-range ordered carbon layers are virtually parallel to the tube axis. Moreover, the spacing between each layer was found to be approximately 0.34 nm, which is consistent with the ideal basal plane distance of a graphite structure. The higher crystallinity of the regularly arranged graphite layers, as compared to that in Figure 2b, is attributed to the relatively high formation temperature. At 600 °C, the atmosphere a_C is 440, which is much smaller than that (9250) at 500 °C. As a result, the carbon deposition rate (from the atmosphere) on the catalyst particle is sufficiently low to ensure the growth of the multiwall CNT, in contrast to the solid carbon nanorod violently extruded from the catalyst particle at 500 °C. Moreover, as shown in Figure 3a, the catalyst with a diameter of approximately 30 nm is encapsulated in the CNT, unlike that illustrated in Figure 2c.

Figure 4a shows the HRTEM micrograph of the nanosized carbon produced at 700 °C; bundles of single-wall CNTs can be clearly recognized. Many tiny nanoparticles (with a diameter

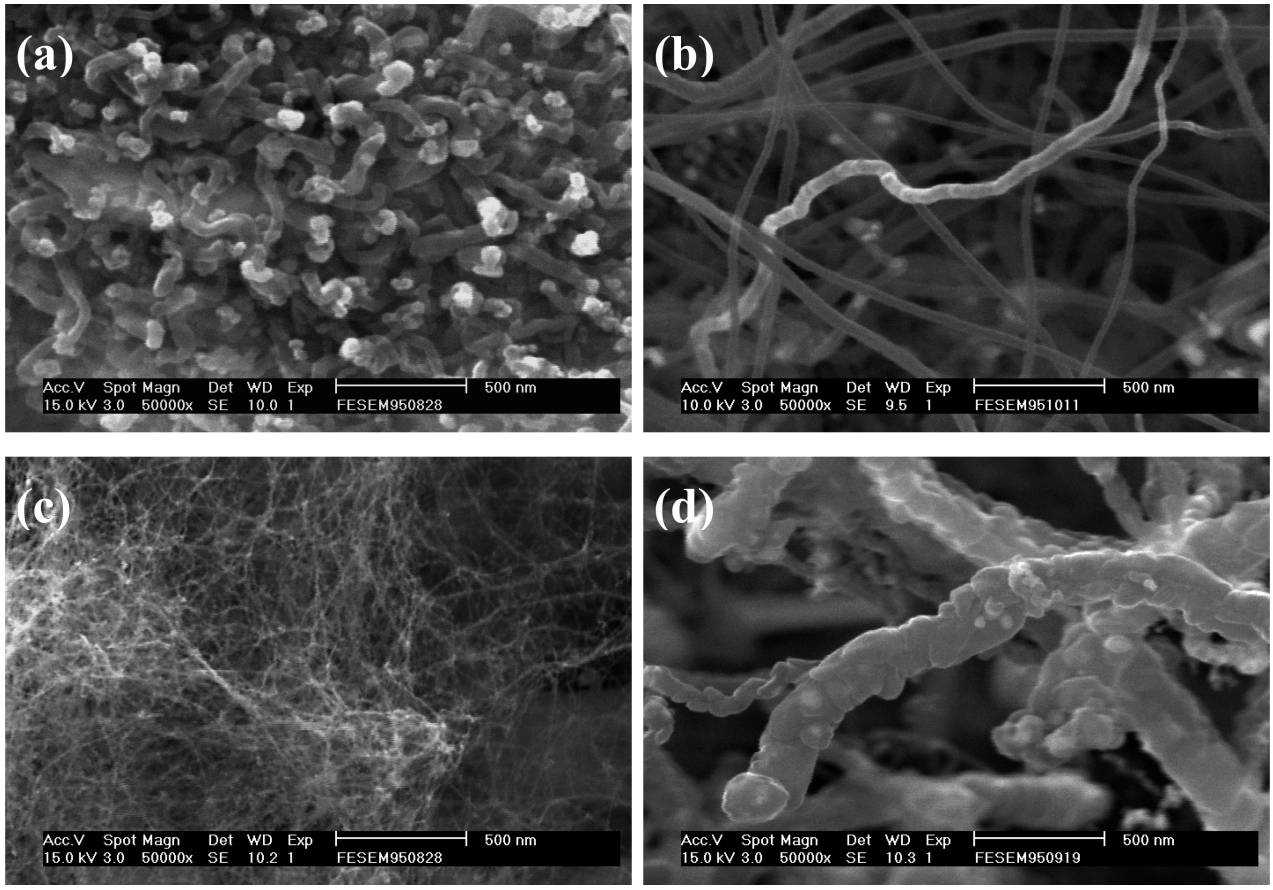

Figure 1. Surface morphologies of the 304 L stainless steels after being exposed to the $CO-CO_2$ mixed gas for 30 h at (a) 500, (b) 600, (c) 700, and (d) 800 °C.

of only about 5 nm), which are believed to catalyze the formation of the CNTs, can be observed in Figure 4b. EDS analyses confirmed that the particle also consisted of 89 wt % Fe and 11 wt % Ni. It was found that the particle size of the catalyst gradually decreases, but the particle number increases, from 500 to 700 °C. When the dramatic reduction of a_C (as shown in Table 2) is taken into account, the carbon deposition amount per catalyst particle is much lower at a higher temperature. As a result, single-wall CNTs were formed. It should be noted that the formation temperature of single-wall CNTs, say 700 °C, is remarkably lower than that reported in the literature.[29,30]

Figure 5a shows the microstructure of the carbon deposited at 800 °C, which is quite different from the fiber type of carbon structure observed at 500−700 °C. It is interesting to find that the sticks are actually composed of many connected metal encapsulated carbon nanoballs; each has a diameter of approximately 65 nm, as shown in Figure 5b. The metal particle with a diameter of approximately 35 nm had a chemical composition similar to those of the 500−700 °C produced particles. Since the a_C is only 5 at 800 °C, the tendency (or rate) of carbon deposition from the atmosphere is pretty low; consequently, the temperature and carbon concentration gradients across the catalyst particles could be ignored. As a result, the tubular structure cannot form in this case; the deposited carbon atoms just precipitate uniformly around the surface of catalyst particles to lower the overall free energy. Figure 5b also reveals a great crystallinity of the deposited graphite layers, showing obvious bending contours in the TEM image. At a higher formation temperature, the carbon atoms have sufficiently high mobility to stack on energy-favoring positions. Therefore, as demonstrated in this paper, the higher the reaction temperature, the better the crystallinity of the deposited carbon that can be obtained. It should also be noted that the diameter of the catalyst particles produced at 800 °C is much bigger than that at 700 °C, suggesting that a distinct reaction mechanism of metal dusting may operate at the higher temperature. This phenomenon could be explained by considering two factors: (1) The iron decomposed from cementite (M_3C) does not form fine particles but agglomerates to bulks or even a continuous layer when the reaction temperature is higher than 700 °C.[20,31] (2) For an alloy containing higher than 5 wt % Ni,[32] especially at an elevated temperature,[20] no metastable M_3C carbide can be developed. The alloy is destroyed by direct inward growth of graphite into the oversaturated solid solution. The stress generated during graphite precipitation fractures the alloy surface and dislodges metal particles, which are considerably bigger than those produced via the mechanism of M_3C decomposition.[20,23]

Laser ablation is a known technique to prepare diamond films[33] and single-wall CNTs with high purity and uniformity,[34] while arc discharge[35] is another conventional method that can produce carbon soot. The carbon soot is a mixture of graphite, carbon whiskers, fullerenes, and catalysts; therefore, an extensive postpurification process is needed to get a particular carbon product.[36] CVD is a popular and well-established process of growing carbon nanomaterials on a large scale; variable parameters (such as precursor, temperature, pressure, and catalysts) have to be carefully controlled to deposit a desired carbon structure. Carbon nanofibers, single-wall CNTs, multiwall CNTs, and diamondlike carbon have been successfully deposited.[36] Table 2 summarizes the various forms of nanosized carbon materials that can be prepared via our metal dusting process. The metal dusts produced from a 304 L coupon in the

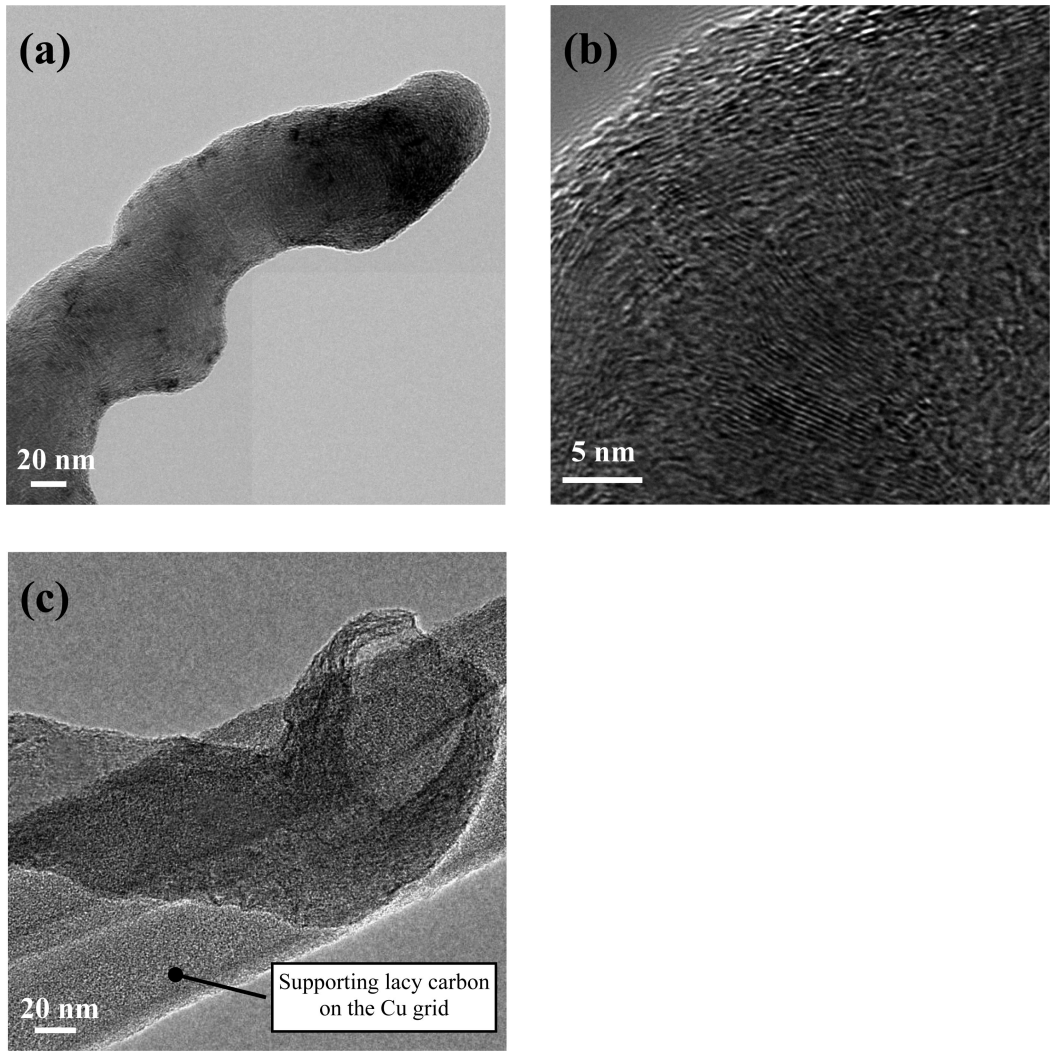

Figure 2. (a, c) Low- and (b) high-magnification HRTEM micrographs of a carbon nanorod prepared at 500 °C by a metal dusting process. (a) Ttail region; (c) tip region.

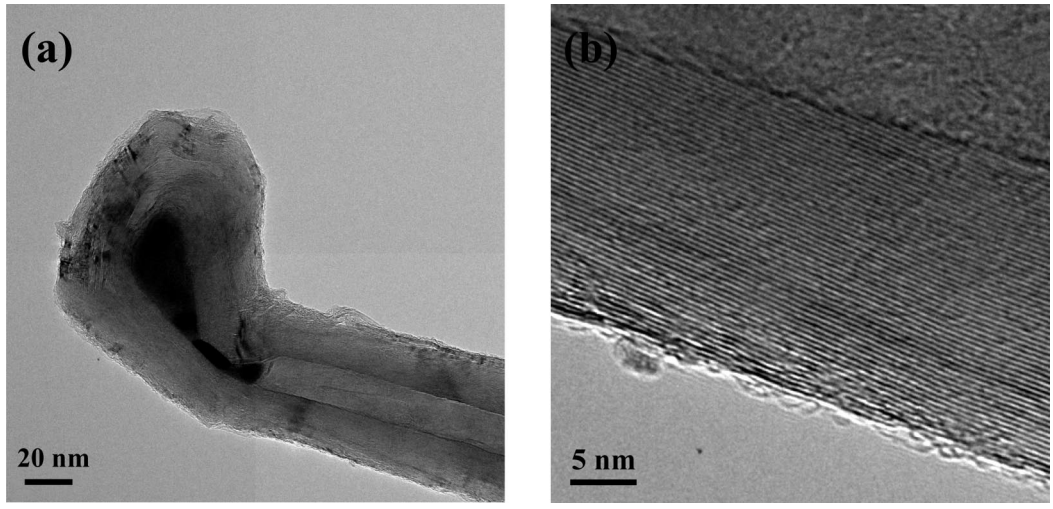

Figure 3. (a) Low- and (b) high-magnification HRTEM micrographs of a multiwall carbon nanotube prepared at 600 °C by a metal dusting process.

temperature range have different diameters (but with similar chemical composition); with appropriate atmospheric carbon activity, the growth of a variety of carbon nanostructures that was catalyzed by the produced metal dusts has been demonstrated.

4. Conclusions

An efficient and simple metal dusting process, in which a blasted 304 L stainless steel coupon and $CO-CO_2$ mixed gas

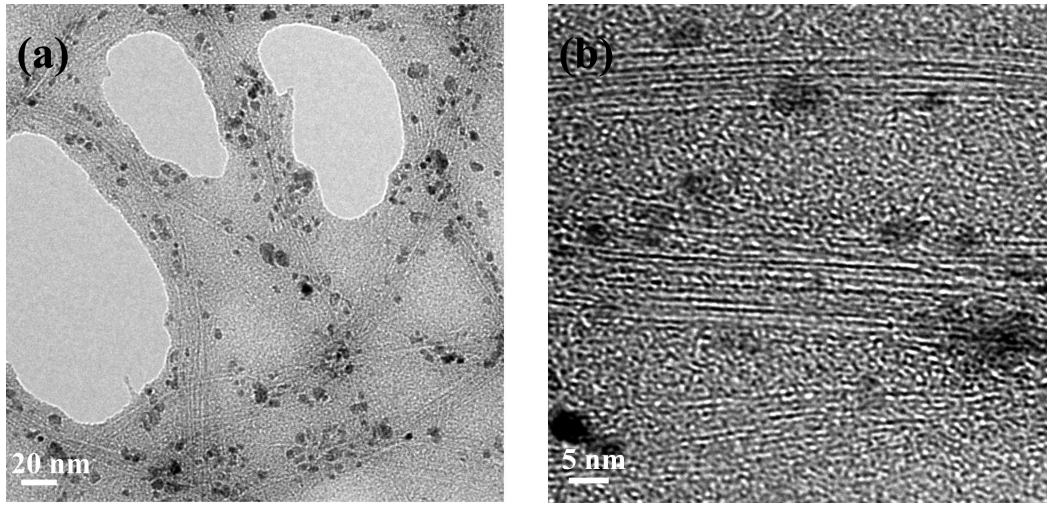

Figure 4. (a) Low- and (b) high-magnification HRTEM micrographs of bundles of single-wall carbon nanotubes prepared at 700 °C by a metal dusting process.

TABLE 2: Effects of Carbon Activity and Diameters of the Metal Dusting-Produced Catalyst Particles on the Types of Nanosized Carbon Materials Prepared[a]

temperature (°C)	500	600	700	800
carbon activity	9250	440	39	5
avg diameter of catalyst particles produced (nm)	70	30	5	35
type of nanosized carbon material deposited	nanorod	multiwall CNT	single-wall CNT	nanoball
diameter of nanosized carbon material (nm)	80	60	10	65

[a] The metal dusting process was performed in $CO-CO_2$ mixed gas (35:1) in the 500−800 °C temperature range.

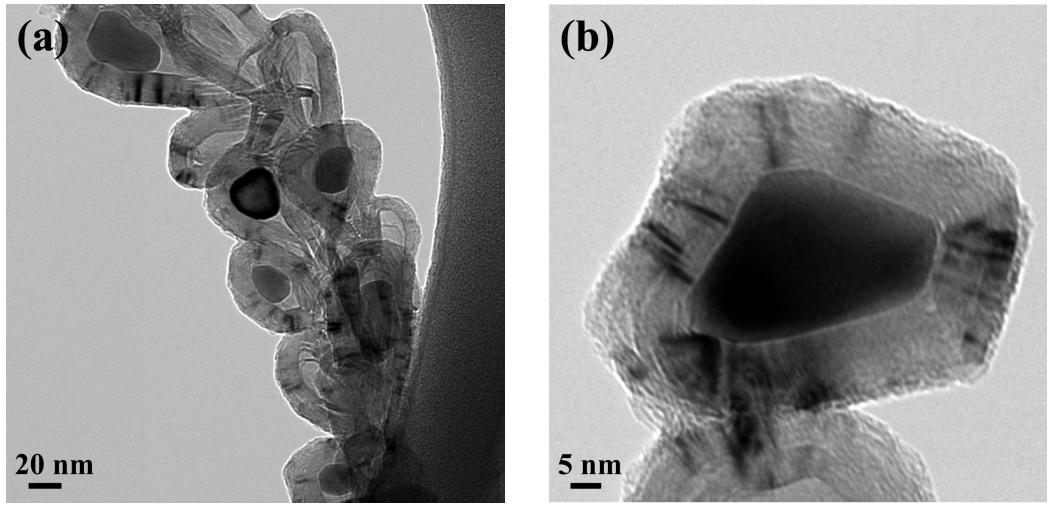

Figure 5. (a) Low- and (b) high-magnification HRTEM micrographs of a stick of connected metal encapsulated carbon nanoballs prepared at 800 °C by a metal dusting process.

are the only reactants needed, to prepare different types of nanosized carbon has been proposed. During the process, fresh Fe−Ni nanoparticles are produced spontaneously from the steel, and these consequently catalyze the growth of nanosized carbon materials. However, the particle size and amount of the catalyst evidently depend on the reaction conditions. With the dramatic decrease of a_C from 9250 (at 500 °C) to 5 (at 800 °C), different nanosized carbon structures, such as nanorods, multiwall CNTs, single-wall CNTs, and metal encapsulated carbon nanoballs, can be constructed.

Acknowledgment. We thank the National Science Council of the Republic of China and the Atomic Energy Council for financially supporting this research under Contract NSC 95-2623-7-006-009-NU.

References and Notes

(1) Iijima, S. *Nature* **1991**, *354*, 56.
(2) Saito, R.; Fujita, M.; Dresselhaus, G.; Dresselhaus, M. S. *Appl. Phys. Lett.* **1993**, *60*, 2204.
(3) Ruoff, R. S.; Lorents, D. C. *Carbon* **1995**, *33*, 925.
(4) Trans, S. J.; Verschueren, A. R. M.; Dekker, C. *Nature* **1998**, *393*, 49.
(5) Mintmire, J. W.; Dunlap, B. I.; White, C. T. *Phys. Rev. Lett.* **1992**, *68*, 631.
(6) Maurin, G.; Bousquet, C.; Henn, F.; Bernier, P.; Almairac, R.; Simon, B. *Chem. Phys. Lett.* **1999**, *312*, 14.
(7) Frackowiak, E.; Metenier, K.; Bertagna, V.; Beguin, F. *Appl. Phys. Lett.* **2000**, *77*, 2421.
(8) Bessel, C. A.; Laubernds, K.; Rodriguez, N. M.; Baker, R. T. K. *J. Phys. Chem. B* **2001**, *105*, 1115.
(9) Dillon, A. C.; Jones, K. M.; Bekkedahl, T. A.; Kiang, C. H.; Bethune, D. S.; Heben, M. J. *Nature* **1997**, *386*, 377.

(10) Wang, Q.; Challo, S. R.; Sholl, D. S.; Johnson, J. K. *Phys. Rev. Lett.* **1999**, *82*, 956.
(11) Ebbessen, T. W.; Ajayan, P. M. *Nature* **1992**, *358*, 220.
(12) Guo, T.; Nikolaev, P.; Thess, A.; Colbert, D. T.; Smalley, R. E. *Chem. Phys. Lett.* **1995**, *243*, 49.
(13) Yacaman, M. J.; Yoshida, M. M.; Rendon, L. *Appl. Phys. Lett.* **1993**, *62*, 202.
(14) Zhang, J.; Schneider, A.; Inden, G. *Corros. Sci.* **2003**, *45*, 1329.
(15) Chun, C. M.; Mumford, J. D.; Ramanarayanan, T. A. *J. Electrochem. Soc.* **2002**, *149*, B348.
(16) Lin, C. Y.; Tsai, W. T. *Mater. Chem. Phys.* **2003**, *82*, 929.
(17) Hochman, R. F. In *Proceedings of the 4th International Congress on Metallic Corrosion*; Hammer, N. E., Ed.; National Association of Corrosion Engineers: Houston, TX, 1972.
(18) Nava Paz, J. C.; Grabke, H. J. *Oxid. Met.* **1993**, *39*, 437.
(19) Grabke, H. J. *Mater. Corros.* **1998**, *49*, 303.
(20) Grabke, H. J. *Mater. Corros.* **2003**, *54*, 736.
(21) Chun, C. M.; Mumford, J. D.; Ramanarayanan, T. A. *Mater. Corros.* **1999**, *50*, 634.
(22) Chun, C. M.; Ramanarayanan, T. A. *Oxid. Met.* **2004**, *62*, 71.
(23) Chun, C. M.; Ramanarayanan, T. A. *J. Electrochem. Soc.* **2005**, *152*, B169.
(24) Sinnott, S. B.; Andrews, R.; Qian, D.; Rao, A. M.; Mao, Z.; Dickey, E. C.; Derbyshire, F. *Chem. Phys. Lett.* **1999**, *315*, 25.
(25) Baker, R. T. K.; Barber, M. A.; Harris, P. S.; Feates, F. S.; Waite, R. J. *J. Catal.* **1972**, *26*, 51.
(26) Baker, R. T. K. *Carbon* **1989**, *27*, 315.
(27) Nielsen, J. R.; Trimm, D. L. *J. Catal.* **1977**, *48*, 155.
(28) Grabke, H. J.; Bracho-Troconis, C. B.; Müller-Lorenz, E. M. *Mater. Corros.* **1994**, *45*, 215.
(29) Jung, M.; Eun, K. Y.; Lee, J. K.; Baik, Y. J.; Lee, K. R.; Park, J. W. *Diamond Relat. Mater.* **2001**, *10*, 1235.
(30) Jang, Y. T.; Ahn, J. H.; Lee, Y. H.; Ju, B. K. *Chem. Phys. Lett.* **2003**, *372*, 745.
(31) Schneider, A. *Corros. Sci.* **2002**, *44*, 2353.
(32) Pippel, E.; Woltersdorf, J.; Grabke, H. J. *Mater. Corros.* **2003**, *54*, 747.
(33) Yoshimoto, M.; Yoshida, K.; Maruta, H.; Hishatani, Y.; Koinuma, H.; Nishio, S.; Kakihana, M.; Tachibana, T. *Nature* **1999**, *399*, 340.
(34) Thess, A.; Lee, R.; Nikolaev, P.; Dai, H.; Petit, P.; Robert, J.; Xu, C.; Lee, Y. H.; Kim, S. G.; Rinzler, A. G.; Colbert, D. T.; Scuseria, G. E.; Tománek, D.; Fischer, J. E.; Smalley, R. E. *Science* **1996**, *273*, 483.
(35) Kroto, H. W.; Heath, J. R.; O'Brien, S. C.; Curl, R. F.; Smalley, R. E. *Nature* **1985**, *318*, 162.
(36) Sharon, M; Sharon, M. *Synth. React. Inorg., Met.-Org., Nano-Met. Chem.* **2006**, *36*, 365.

JP803202M